Supplement -- **Fus3-triggered Tec1 degradation modulates mating transcriptional output during the pheromone response**

Song Chou[1,#], Su Zhao[2,#], You Song[2,4], Haoping Liu[1,3,] *and Qing Nie[2,3,*]

[1]Department of Biological Chemistry,
[2]Department of Mathematics,
[3]Center for Complex Biological Systems,
University of California, Irvine,
Irvine, CA 92697

[4]College of Software,
Beihang University,
Beijing 100083, China

#Equal contribution

*Corresponding authors: h4liu@uci.edu and qnie@math.uuci.edu

Model and equations

The model aims to study emergent properties arising from interactions and regulations among several transcription factors in the yeast mating pathway. The system consists of Tec1, Ste12, Dig1, Dig2, PRE, TCS, and their reaction products. Dig1 in the system is not explicitly modeled, and only the complex Ste12/Dig1 is included in the system. The system is activated by pheromone through active Fus3 and Kss1 that in turn inhibit Dig1 and Dig2 (Cook, 1996; Tedford, 1997), and positively regulate Tec1 degradations (Chou, 2004). And the *TEC1* expression is also positively regulated by the PRE signal (Oehlen, 1998). For simplicity, the active Fus3 and Kss1 are assumed to be proportional to the pheromone level (Sabbagh, 2001) (*posters and keynote presentation by Roger Brent, et al. at ICSB07).* The biochemical reactions along with the rate constants are presented in Figure S1. The corresponding mass action equations take the following form:

(1) $\frac{dT}{dt} = -k_{on} T \bullet S + k_{off} N - K_{\deg}(U)T + P_T(\bar{C})$

(2) $\frac{dS}{dt} = -k_{on} T \bullet S + k_{off} N + J_{\deg}(U)N - l_{on} G \bullet S + l_{off} M + L_{\deg}(U)B + I_{\deg}(U)F$

(3) $\frac{dG}{dt} = -l_{on} G \bullet S + l_{off} M$

(4) $\frac{dM}{dt} = l_{on} G \bullet S - l_{off} M - w_{on} M \bullet R_1 + w_{off} A$

(5) $\frac{dN}{dt} = k_{on} T \bullet S - k_{off} N - J_{\deg}(U)N - v_{on} N \bullet R_1 + v_{off} B - z_{on} N \bullet R_2 + z_{off} F$

(6) $\frac{dA}{dt} = w_{on} M \bullet R_1 - w_{off} A - w_d(U,V)A$

(7) $\frac{dR_1}{dt} = -w_{on} M \bullet R_1 + w_{off} A - v_{on} N \bullet R_1 + v_{off} B + L_{\deg}(U)B$

(8) $\frac{d\bar{A}}{dt} = w_d(U,V)A - W_{\deg 1}\bar{A}$

(9) $\frac{dB}{dt} = v_{on} N \bullet R_1 - v_{off} B - v_d(U,V)B - L_{\deg}(U)B$

(10) $\frac{d\bar{B}}{dt} = v_d(U,V)B - W_{\deg 2}\bar{B}$

(11) $\frac{dF}{dt} = z_{on} N \bullet R_2 - z_{off} F - z_d(U,V)F - I_{\deg}(U)F$

(12) $\frac{dR_2}{dt} = -z_{on} N \bullet R_2 + z_{off} F + I_{\deg}(U)F$

(13) $\frac{d\bar{F}}{dt} = z_d(U,V)F - W_{\deg 3}\bar{F}$

Below is the list of the notations and symbols used in the above equations

T: Tec1.
S: Ste12/Dig1
G: Dig2.
M: Ste12/Dig1/Dig2 complex
N: Ste12/Dig1/Tec1 complex
R_1: PRE binding site
R_2: TCS binding site
A: PRE/Ste12/Dig1/Dig2 complex
B: PRE/Ste12/Dig1/Tec1 complex
F: TCS/Ste12/Dig1/Tec1 complex
$\bar{A}$: Active form PRE/Ste12/Dig2 complex
$\bar{B}$: Active form of PRE/Ste12/Tec1 complex

$\overline{F}$: Active form of TCS/Ste12/Tec1 complex

The PRE signal is $\overline{C} \equiv \overline{A} + \overline{B}$ and the TCS signal is $\overline{F}$. The experimentally measurable Tec1 level is the sum of all complexes involving Tec1. The total Ste12 and total Dig2 levels are measured similarly:

$$\text{Tec1}_{\text{total}} = T + N + F + \overline{F} + B + \overline{B}$$

$$\text{Ste12}_{\text{total}} = S + M + A + \overline{A} + N + F + \overline{F} + B + \overline{B}$$

$$\text{Dig2}_{\text{total}} = G + M + A + \overline{A}$$

The input active Fus3 (U) and active Kss1 (V) are chosen as two given functions in terms of time:

$$U(\alpha,t) = u_0 + \frac{k_0\alpha}{b_0+\alpha}\overline{U}(t) \qquad \overline{U}(t) = \begin{cases} 0 & [\text{ before adding } \alpha-\text{factor (pheromone) }] \\ \dfrac{t^{index1}}{t^{index1}+\text{constant1}} & [\ t \geq 0\ ] \end{cases}$$

$$V(\alpha,t) = v_0 + \frac{k_0\alpha}{b_0+\alpha}\overline{V}(t) \qquad \overline{V}(t) = \begin{cases} 0 & [\text{ before adding } \alpha-\text{factor (pheromone) }] \\ \dfrac{t^{index2}}{t^{index2}+\text{constant2}} & [\ 0 \leq t \leq t_0\ ] \\ \dfrac{t^{index2}}{t^{index2}+\text{constant2}} - v_1\dfrac{(t-t_0)^{index3}}{(t-t_0)^{index3}+\text{constant3}} & [\ t \geq t_0\ ] \end{cases}$$

where the variable α is the strength of α-factor (pheromone) with a unit *nM*. The expressions of Fus3 and Kss1 mimic experimentally observed temporal dynamics for Fus3 and Kss1's response to pheromone (Sabbagh, 2001). It is also consistent with previous simulations on the dynamics of active Fus3 (Wang, 2006). The level of active Fus3 and Kss1 are assumed to be proportional to the level of pheromone based on previous experimental observation (Sabbagh, 2001) (*posters and keynote presentation by Roger Brent, et. al at ICSB0).* The two functions are plotted in Figure S2.

The degradation of Tec1 is positively regulated by Fus3 (Bao, 2004; Chou, 2004). Tec1 degradation rates are modeled in terms of the Hill function of Fus3:

$$K_{\text{deg}}(U) = K_{\text{deg min}} + \frac{K_{\text{deg max}}(\gamma U)^n}{1+(\gamma U)^n} \qquad J_{\text{deg}}(U) = \frac{J_{\text{deg max}}(\gamma U)^n}{1+(\gamma U)^n}$$

$$L_{\text{deg}}(U) = \frac{L_{\text{deg max}}(\gamma U)^n}{1+(\gamma U)^n} \qquad I_{\text{deg}}(U) = I_{\text{deg min}} + \frac{I_{\text{deg max}}(\gamma U)^n}{1+(\gamma U)^n}$$

where $K_{\text{deg min}}$ and $I_{\text{deg min}}$ represent low basal levels of degradation without any pheromone stimulation. The inhibition of Fus3 and Kss1 on Dig1 is modeled through activation of the inactive complex inhibited by Dig1 using the activated function:

$$w_{\mathrm{d}}(U,V)=W_{\mathrm{d\,max}1}U+W_{\mathrm{d\,max}2}V$$
$$v_{\mathrm{d}}(U,V)=V_{\mathrm{d\,max}1}U+V_{\mathrm{d\,max}2}V$$
$$z_{\mathrm{d}}(U,V)=\frac{Z_{\mathrm{d\,max}1}(\gamma_1 U)^{n_1}}{1+(\gamma_1 U)^{n_1}}+\frac{Z_{\mathrm{d\,max}2}(\gamma_1 V)^{n_1}}{1+(\gamma_1 V)^{n_1}}$$

As observed in the experiment, there exists a positive feedback on Tec1 expression (Bao, 2004) from the mating signal. So we also assume Tec1 is positively regulated by the mating signal.

$$P_T(\bar{C})=\frac{P_{T\max C}(\gamma_2\bar{C})^{n_2}}{1+(\gamma_2\bar{C})^{n_2}} \qquad \bar{C}\equiv\bar{A}+\bar{B}$$

Results

Temporal dynamics of all complexes

The parameters of the systems in Figure 1 are chosen based on a biochemical analysis of various complexes in (Chou, 2006). The initial concentrations used in Fig. 1 of the paper are listed in Table 1, and the reaction rates and feedback parameters for Fig. 1 are listed in Table 2.

Figure S2A plots the concentration of temporal dynamics of each complex in the system for the wild-type case shown in Fig. 1B of the paper. Figure S2B plots the total level of Dig2 and Ste12, Tec1, and PRE and TCS outputs. The total Dig2 and total Ste12 levels are constant in time, behaving like the experiment. The nonlinear response of total Tec1 is consistent with the experimental observation, and the specificity of PRE output agrees well with the experiments (Bao, 2004; Chou, 2004).

Effect of Tec1 degradation

Figure S3 shows how the level of degradation of Tec1 affects TCS outputs. We varied the mean strength of Tec1 degradation in the model. As expected, Tec1 degradation strength dictates the level of Tec1, which in turn controls the TCS-*lacZ* level. For the case of zero degradation of Tec1 in the model, which correlates to the stable Tec1^{T273V}, the Tec1 level monotonically increases from the start while the fold change of TCS-*lacZ* always increases in response to pheromone. On the other extreme, when Tec1 degradation is large, the TCS-*lacZ* level decreases after pheromone induction. In both cases, the simulated results are in agreement with the experimental data (Chou, 2004) (Bao, 2004).

Strategy one -- Ste12/Dig1/Dig2 is more effective in activating mating gene transcription than Tec1/Ste12/Dig1

The ranges of randomly chosen parameters in Fig. 2 of the paper are listed in Table 2. Figure S4A shows that the qualitative pattern of PRE outputs under various mutations presented in Fig. 1C remains unchanged as long as w_d is larger than v_d. Figure S4B

demonstrates that the strategy remains valid for higher levels of induced pheromone. Figure S4C shows that at this pheromone level, when w_d and v_d are changed to be the same, the system behaves similar to that at the low pheromone level. Figure S4D is the experimental result on the *dig2* deletion at different levels of pheromone to show that the *dig2* effect is independent of pheromone levels.

Strategy two -- Tec1 can sequester Ste12 from forming the Ste12/Dig1/Dig2 complex to reduce the mating transcriptional output when the amount of Ste12 is limiting

The parameters for Figure 1D are listed in Table 3. Figure S5 shows that the qualitative pattern on the PRE outputs under the conditions of stable Tec1 and *tec1* deletion remain the same when the system is induced by different levels of pheromone. In Figure S6, we set the overall activation rate of Fus3 on Ste12 in Tec1/Ste12/Dig1 to be the same as the rate for Ste12 in Ste12/Dig1/Dig2 as in the case in Figure 3. A consistent pattern between panel (A) and panel (B) in Figure S6 suggests that 50 sample points are sufficient to identify the correlation. In both panels (A) and (B), there are few samples satisfying the condition in which both ratio of PRE output for the *tec1* deletion over PRE output for WT (R_1) and ratio of PRE output for WT over PRE output for stable Tec1 (R_2) are greater than 1. As the initial amount of Ste12 decreases, there are more sample points satisfying the condition which resembles the experimental result shown in Figure 1C.

Figure S7 is an example in which more sample points were added around the case which agrees well with the experimental result. The binding affinities are defined as

$$\mathrm{K}_{\mathrm{Tec1|Ste12}} = \frac{k_{on}}{k_{off}},\ \mathrm{K}_{\mathrm{Dig2|Ste12}} = \frac{l_{on}}{l_{off}},\ \mathrm{K}_{\mathrm{Dig2|PRE}} = \frac{w_{on}}{w_{off}},\ \mathrm{K}_{\mathrm{Tec1|PRE}} = \frac{v_{on}}{v_{off}},\ \mathrm{K}_{\mathrm{Tec1|TCS}} = \frac{z_{on}}{z_{off}}$$

In Figure S8, we systematically varied the initial amount of Ste12 to study how it affects strategy two. In Figure S9, we systematically test the condition under which the correlation on affinities for strategy two remains true. Both figures show strategy two is a robust strategy as long as Ste12 is sequestered. In Figure S10, we find that, under the same conditions, the lower the initial amounts of PREs and TCSs were, the fewer the red dots were, however, with a clearer relationship between the two affinities: $\mathrm{K}_{\mathrm{Dig2|PRE}}$ and $\mathrm{K}_{\mathrm{Tec1|PRE}}$. In Figure S11, as the ratio of w_d over v_d increases from 0.5 to 4, the output level of the PRE in wild type stain increases while PRE signals of other cases hardly change. Consequently, the difference in PRE level between the tec1 deletion and the wild type becomes smaller.

References

Bao, M., Schwartz, M. , Gantin, G., Yates III, J., Madhani, H. (2004) Pheromone-Dependent Destruction of the Tec1 Transcription Factor is Required for MAP Kinase Signaling Specificity in Yeast. *Cell*, **119**, 991-1000.

Chou, S., Huang,L., Liu, HP. (2004) Fus3-Regulated Tec1 Degradation through SCF^{Cdc4} Determines MAPK Signaling Specificity during Mating in Yeast. *Cell*, **119**, 1-20.

Chou, S., Lane, S., Liu, HP. (2006) Regulation of Mating and Filamentation Genes by Two Distinct Ste12 Complexes in Sacharomyces cerevisiae. *Molecular and Cellular Biology*, **26**, 4794-4805.

Cook, J.G., Bardwell, L., Kron, S. J., Thorner, J. (1996) Two novel targets of the MAP kinase Kss1 are negative regulators of invasive growth in the yeast Saccharomyces cerevisiae. *Genes Dev*, **10**, 2831-2848.

Oehlen, L., Cross, F. R. (1998) The mating factor response pathway regulates transcription of TEC1, a gene involved in pseudohyphal differentiation of Saccharomyces cerevisiae. *FEBS Lett*, **429**, 83-88.

Sabbagh, W., Jr., Flatauer, L. J., Bardwell, A. J. & Bardwell, L. (2001) Specificity of MAP kinase signaling in yeast differentiation involves transient versus sustained MAPK activation. *Mol Cell*, **8**, 683-691.

Tedford, K., Kim, S., Sa, D., Stevens, K., Tyers, M. (1997) Regulation of the mating pheromone and invasive growth responses in yeast by two MAP kinase substrates. *Curr Biol*, **7**, 228-238.

Wang, X., Hao, N., Dohlman, H.G., Elston, T. C. (2006) Bistability, stochasticity, and oscillations in the mitogen-activated protein kinase cascade. *Biophys J*, **90**, 1961-1978.

Figures and Tables -- Supplement

name	initial value	unit
Tec1	1	μM
Ste12/Dig1	1	μM
Dig2	1	μM
Ste12/Dig1/Dig2	0	μM
Ste12/Dig1/Tec1	0	μM
PRE/Ste12/Dig1/Dig2	0	μM
PRE	0.1	μM
PRE/Ste12/Dig2	0	μM
PRE/Ste12/Dig1/Tec1	0	μM
PRE/Ste12/Tec1	0	μM
TCS/Ste12/Dig1/Tec1	0	μM
TCS	0.1/0.36	μM
TCS/Ste12/Tec1	0	μM

Table 1. The initial concentrations used in Figure 1**.**

name	value	unit	Range of the random selection
k_{on}	10^{-2}	$\mu M^{-1}sec^{-1}$	0.0010~0.1000
k_{off}	10^{-6}	sec^{-1}	
l_{on}	$5x10^{-3}$	$\mu M^{-1}sec^{-1}$	0.0005~0.0500
l_{off}	10^{-6}	sec^{-1}	
v_{on}	$5x10^{-3}$	$\mu M^{-1}sec^{-1}$	0.0005~0.0500
v_{off}	10^{-6}	sec^{-1}	
w_{on}	$5x10^{-3}$	$\mu M^{-1}sec^{-1}$	0.0005~0.0500
w_{off}	10^{-6}	sec^{-1}	
z_{on}	$5x10^{-3}$	$\mu M^{-1}sec^{-1}$	0.0005~0.0500
z_{off}	$2x10^{-5}$	sec^{-1}	
W_{deg1}	$2.5x10^{-5}$	sec^{-1}	
W_{deg2}	$2.5x10^{-5}$	sec^{-1}	
W_{deg3}	$5x10^{-5}$	sec^{-1}	
n	1		
γ	0.4		
γ_1	20		
K_{degmax}	log(2)/(60*2)	sec^{-1}	0.0029~0.0116
J_{degmax}	log(2)/(60*2)	sec^{-1}	0.0029~0.0116
L_{degmax}	log(2)/(60*2)	sec^{-1}	0.0029~0.0116
I_{degmax}	log(2)/(60*2)	sec^{-1}	0.0029~0.0116
K_{degmin}	log(2)/(60*25)	sec^{-1}	$2.3x10^{-4}$~$9.2x10^{-4}$
I_{degmin}	log(2)/(60*25)	sec^{-1}	$2.3x10^{-4}$~$9.2x10^{-4}$
W_{dmax1}	10^{-4}	sec^{-1}	

W_{dmax2}	10^{-4}	sec^{-1}	
V_{dmax1}	$5x10^{-5}$	sec^{-1}	
V_{dmax2}	$5x10^{-5}$	sec^{-1}	
Z_{dmax1}	$5x10^{-5}$	sec^{-1}	
Z_{dmax2}	$5x10^{-5}$	sec^{-1}	
u_0	$5x10^{-3}$	μM	
index1	2.0		
constant1	$6.0x10^{+5}$		
v_0	$5x10^{-3}$	μM	
v_1	0.95		
t_0	40x60	sec^{-1}	
index2	2.0		
index3	2.0		
constant2	$5.0x10^{+5}$		
constant3	$5.0x10^{+6}$		
k_0	1.5568		
b_0	189.1892		
n_2	1		
γ_2	$2x10^{+4}$		
P_{TmaxC}	$5x10^{-3}$	$\mu M\ sec^{-1}$	

Table 2. Rate constants for Figure 1 and the range for randomly selected parameters in Figure 2 and Figure 3.

name	value	unit
k_{on}	0.0039	$\mu M^{-1}sec^{-1}$
l_{on}	0.0005	$\mu M^{-1}sec^{-1}$
v_{on}	0.0002	$\mu M^{-1}sec^{-1}$
w_{on}	0.0014	$\mu M^{-1}sec^{-1}$
z_{on}	0.0181	$\mu M^{-1}sec^{-1}$
K_{degmax}	0.0048	sec^{-1}
J_{degmax}	0.0157	sec^{-1}
L_{degmax}	0.0050	sec^{-1}
I_{degmax}	0.0056	sec^{-1}
K_{degmin}	0.0007	sec^{-1}
I_{degmin}	0.0009	sec^{-1}
Other parameters are the same as in Table 1 and Table 2.		

Table 3. The parameters used for Figure 1D**.**

name	value	unit	Ranges for the random selections
k_{on}	0.0166	$\mu M^{-1}sec^{-1}$	0.00166~0.1660
l_{on}	0.0025	$\mu M^{-1}sec^{-1}$	0.00025~0.0250
v_{on}	0.0007	$\mu M^{-1}sec^{-1}$	0.00007~0.0070
w_{on}	0.0019	$\mu M^{-1}sec^{-1}$	0.00019~0.0190
z_{on}	0.0387	$\mu M^{-1}sec^{-1}$	0.0038~0.3870
K_{degmax}	0.0050	sec^{-1}	0.0025~0.0100
J_{degmax}	0.0079	sec^{-1}	0.0079~0.0158
L_{degmax}	0.0088	sec^{-1}	0.0044~0.0176
I_{degmax}	0.0100	sec^{-1}	0.0050~0.200
K_{degmin}	0.0005	sec^{-1}	0.0002~0.0010
I_{degmin}	0.0008	sec^{-1}	0.0004~0.0016
The other parameters are the same as in Table 1 and Table 2			

Table 4. The range of randomly selected parameters used in Figure S7B**.**

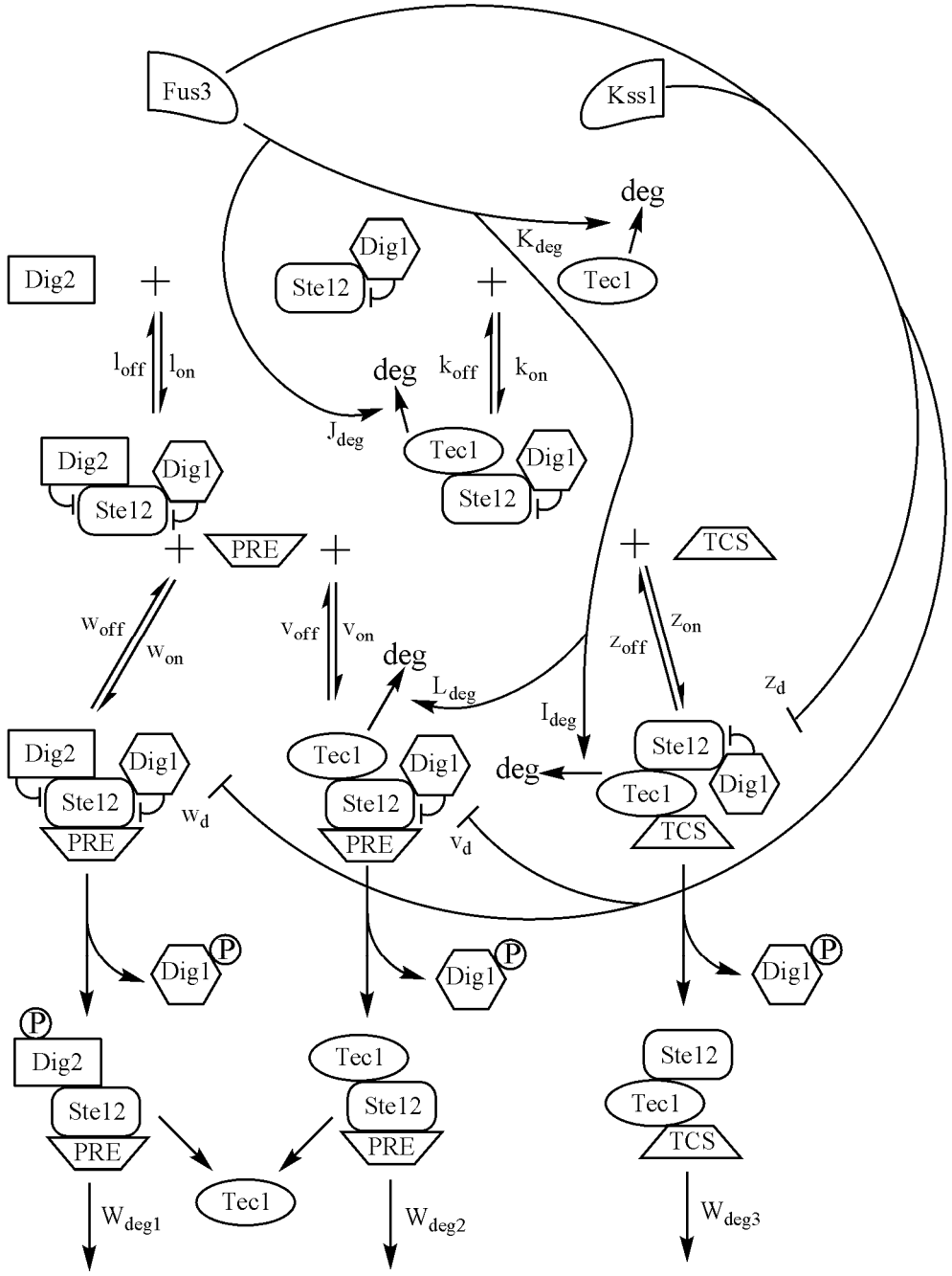

Figure S1. A schematic diagram for biochemical reactions in the model.

A

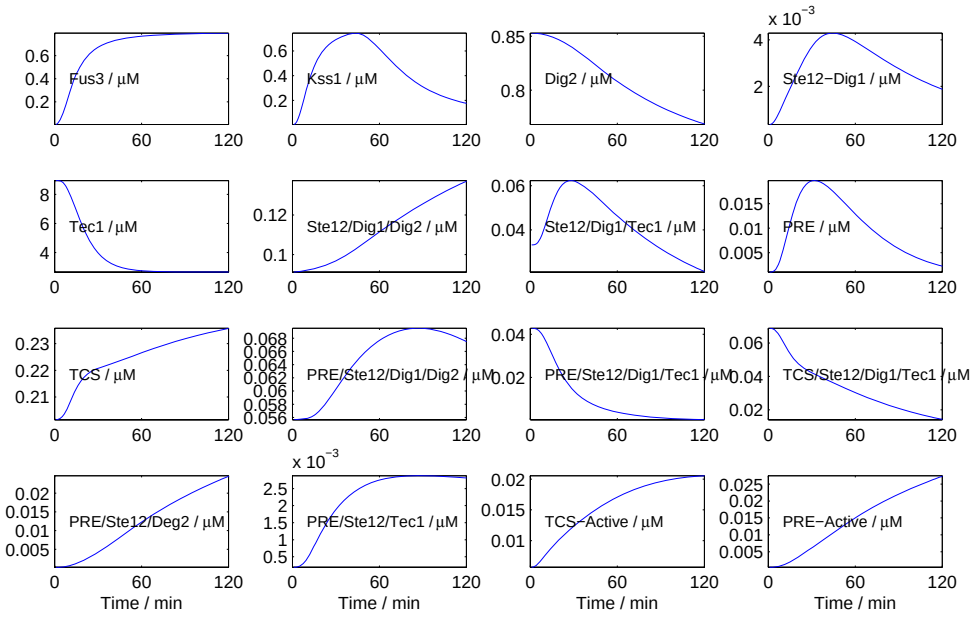

B

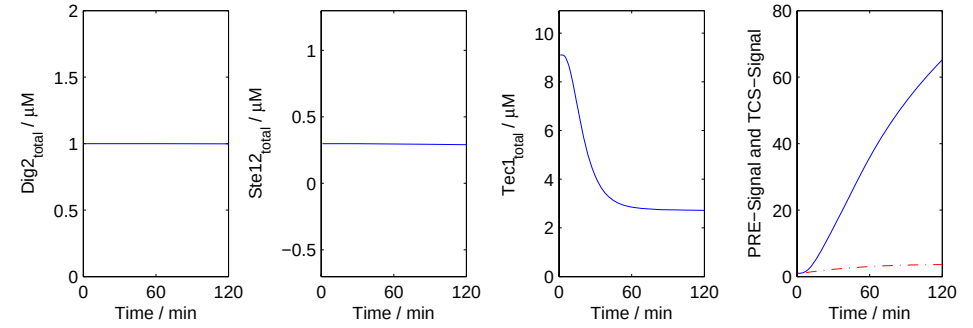

Figure S2. Temporal dynamics of all complexes in the wild type strain shown in Figure 1B of the paper, under 200 nm. (A) Each complex as a function of time; (B) Total Dig2, total Tec1, total Ste12, fold change of the PRE and TCS outputs as functions of time.

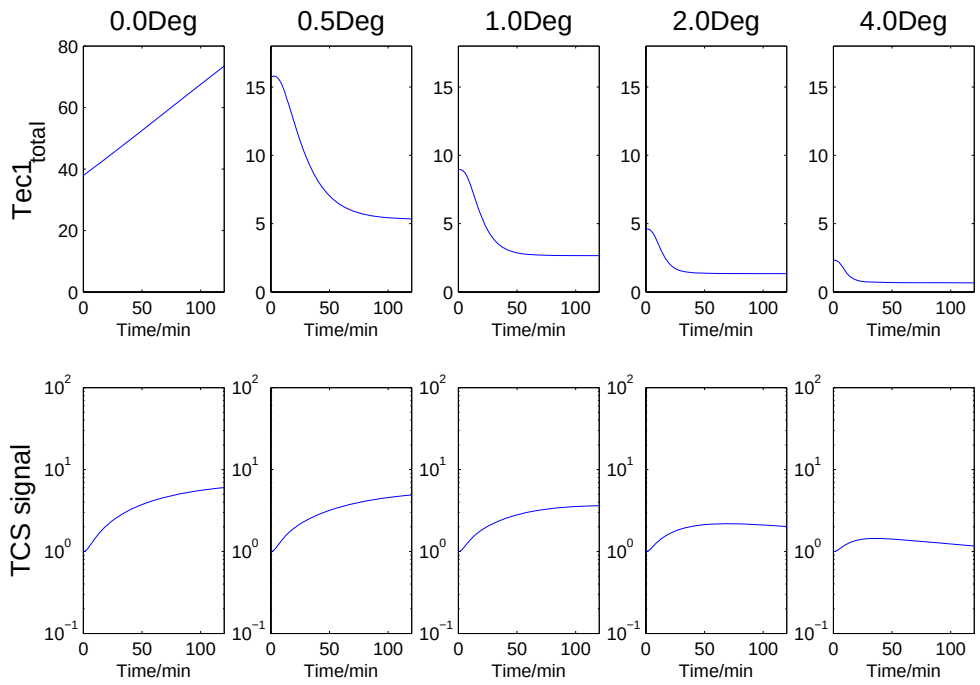

Figure S3. TCS outputs at different Tec1 degradation rates. For each case, the top panel shows the total Tec1 level as a function of time, while the bottom panel shows the corresponding fold change of the TCS output. "xDeg" represents a case in which the mean value of Tec1 degradation is "x" fold of the Tec1 degradation strength used in Figure S2 with all other parameters being same as in Figure S2.

A.

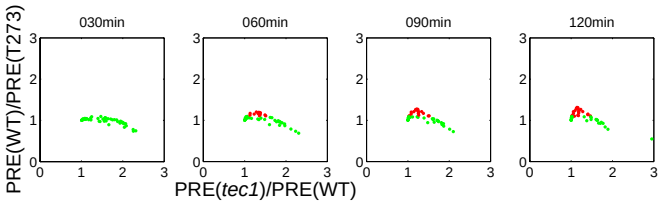

B.

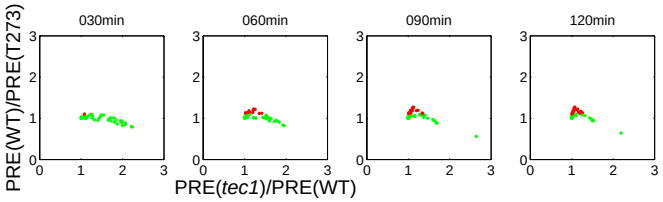

C.

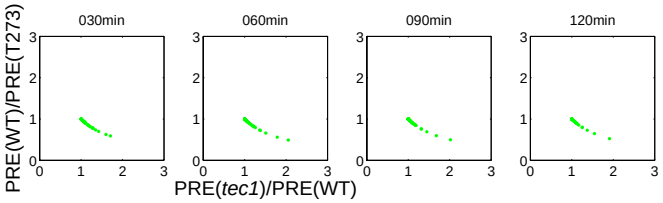

D.

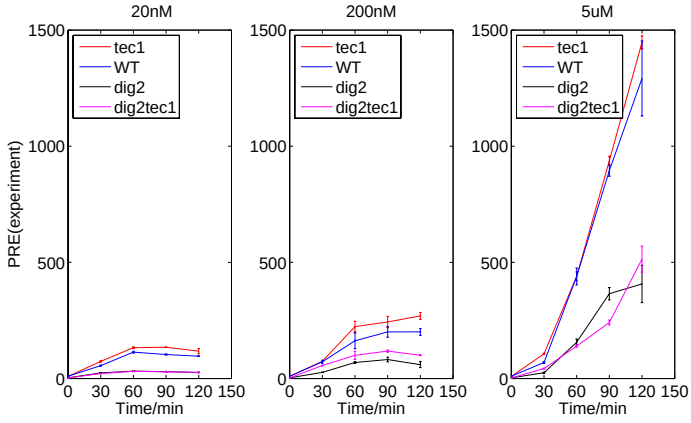

Figure S4 The effect of w_d and the level of induced pheromone using on strategy one. A Red dot represents a case in which the ratio of PRE output for *tec1* deletion over PRE output for WT at 120 min is larger than one *and* the ratio of PRE output for WT over PRE output for stable TEC1 at 120 min is larger than 1.1; a green dot represents a case not satisfying the above condition. (The definitions of red dots and green dots remain the same throughout the rest of the Supplement unless specified otherwise.) (A) The parameters and conditions are the same as Figure 2A, except $w_d = 2v_d$; (B) The parameters and conditions are the same as in (A) except that the induced pheromone is 5 *μM;* (C) The parameters are the same as in (B) except that $w_d = v_d$; (D) The mutation experimental observations shown in Figure 2C but at different levels of induced pheromone.

A.

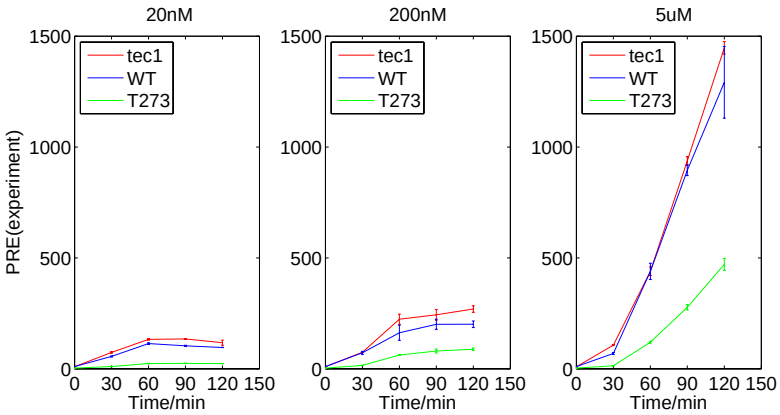

B.

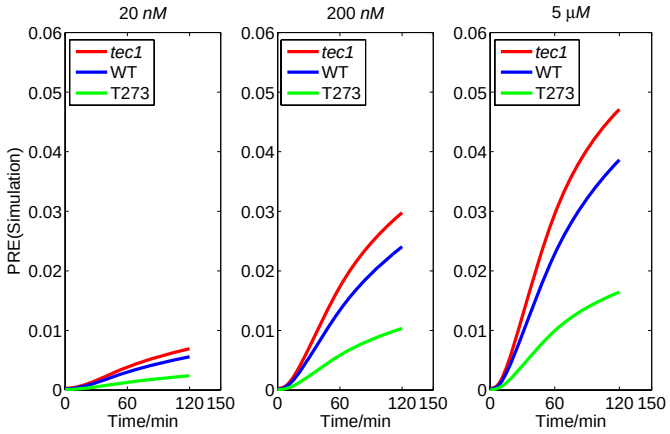

C.

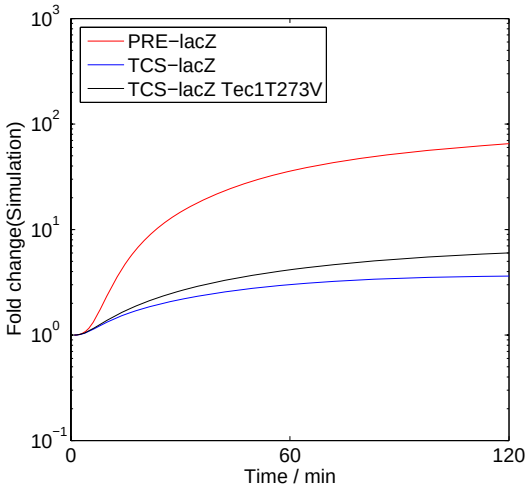

Figure S5. (A) PRE-*lacZ* output as a function of time for WT, the *tec1* deletion and stable *TEC1* strains at different pheromone levels; (B) The parameters used in (B) are the same as in Figure 1B except for the pheromone levels and deletions; (C) The same as in Figure 1B except that the induced pheromone concentration is 200 *nM.*

A.

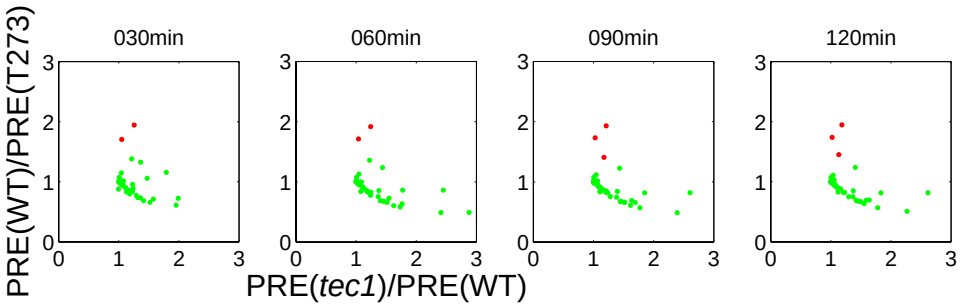

B.

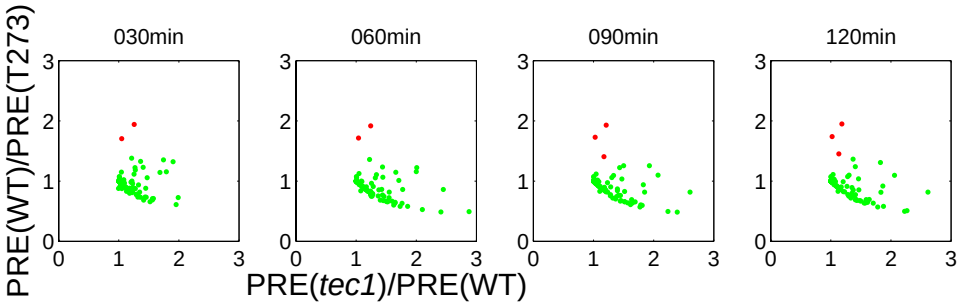

Figure S6. A comparison between a case with 50 sample points and a case with 100 sample points, with the same parameters as in Figure 3. (A) 50 sample points; (B) 100 sample points.

A.

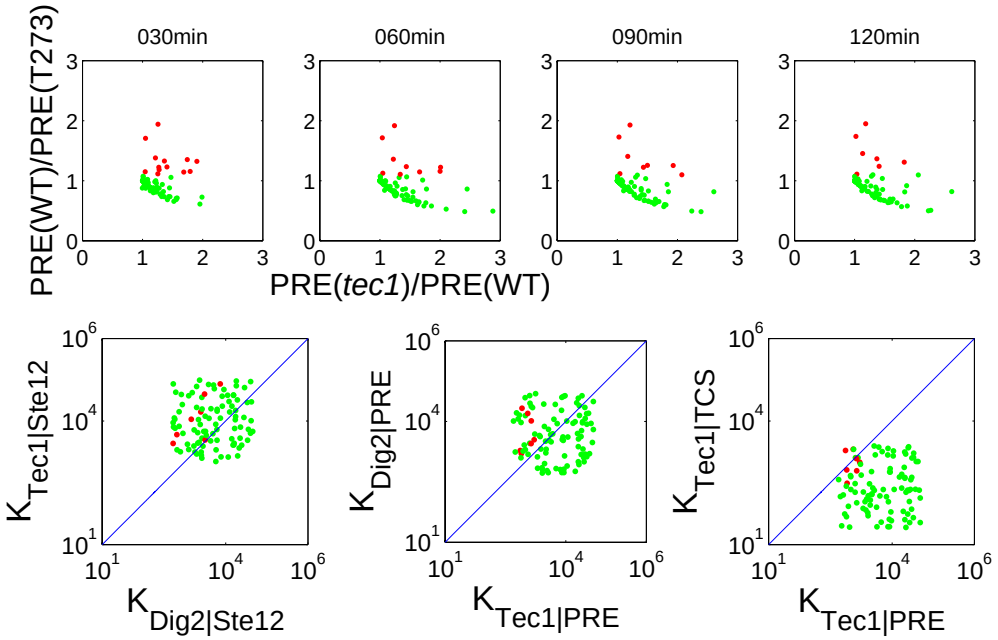

B.

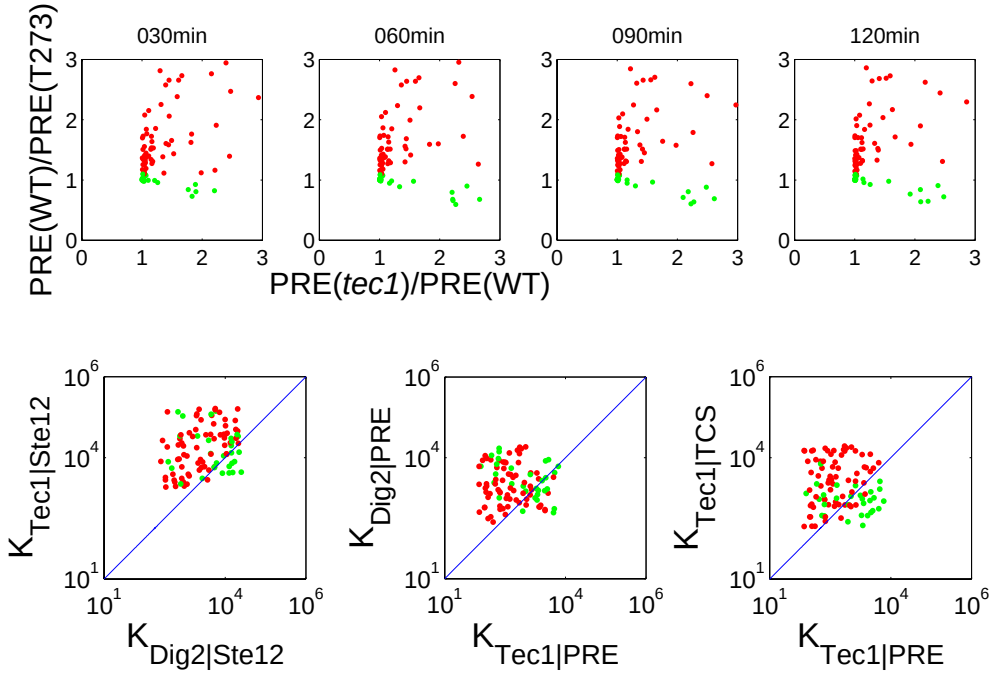

Figure S7. Clustering the sample points around where the experimental observation is realized. (A) 100 sample points whose parameters are chosen based on the range in Table 2; (B) After one set of parameter (see Table 4) in (A) is selected for the pattern resembling the experimental observation, another 100 sample points are randomly selected centering on this set of parameters.

A.

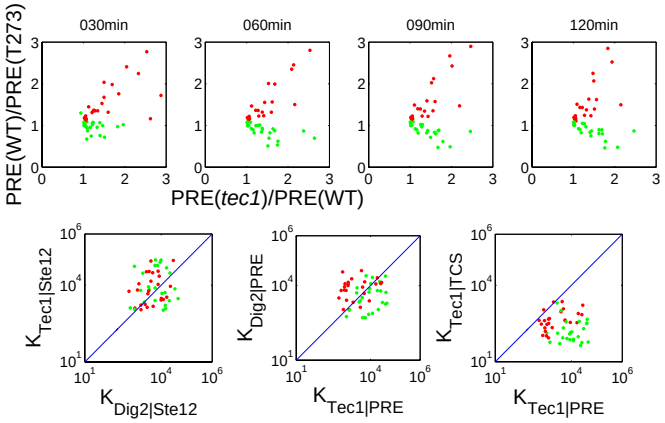

B.

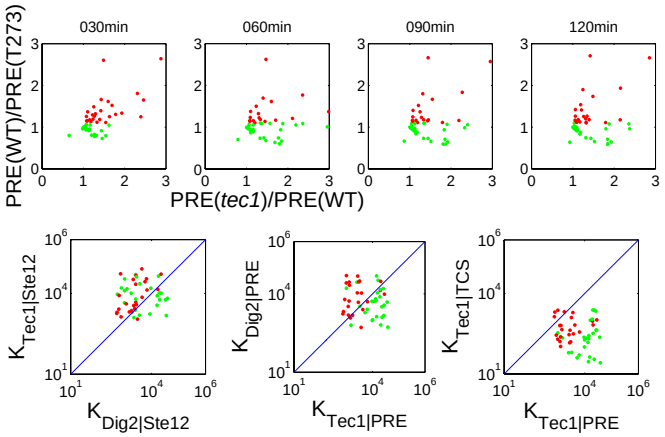

C.

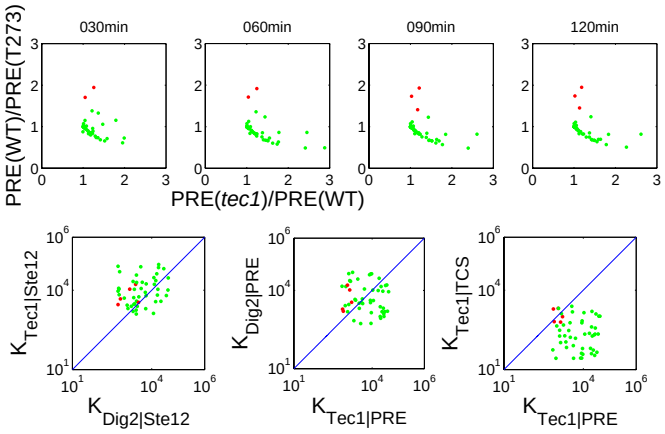

Figure S8. The correlation between the affinity rates at the various levels of initial Ste12. The parameters used in the simulations and definition of the sample points are the same as those in Figure S7 except the initial amount of Ste12. (A) [Ste12] = 0.05 μM and 50 sample points; (B) [Ste12] = 0.15 μM and 50 sample points; (C) [Ste12] = 0.30 μM and 50 sample points.

A.

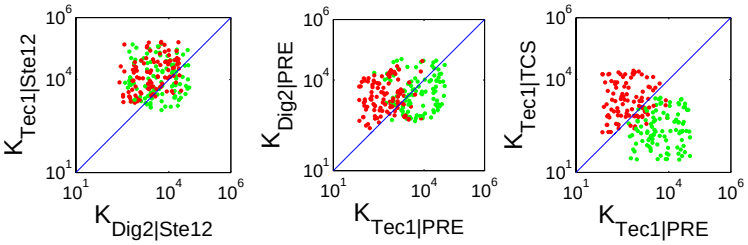

B.

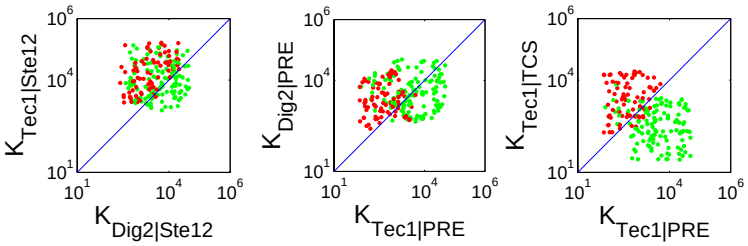

C.

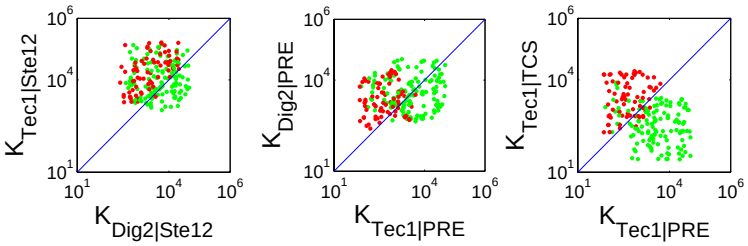

D.

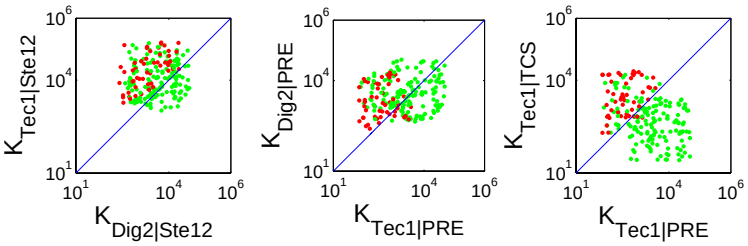

E.

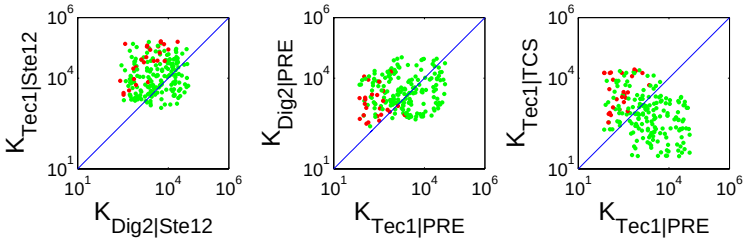

Figure S9. The correlation between affinity rates using different criteria defining the red dots. All other conditions are the same as in Figure 3. A red dot represents a case in which the ratio of PRE output for the *tec1* deletion over PRE output for WT at 120 min is larger than one *and* the ratio of PRE output for WT over PRE output for stable *TEC*1 at 120 min is larger than (A) 1.0; (B) 1.1; (C) 1.2; (D) 1.4; (E) 2.0; a green dot represents points not satisfying the condition.

A.

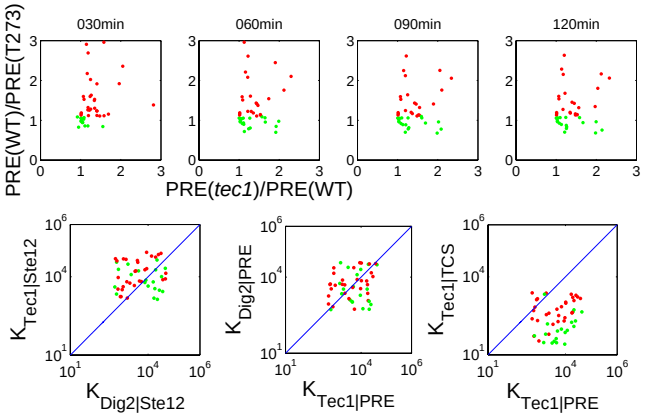

B.

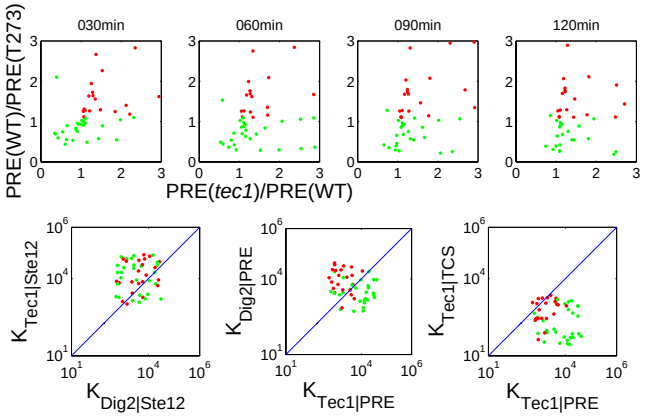

C.

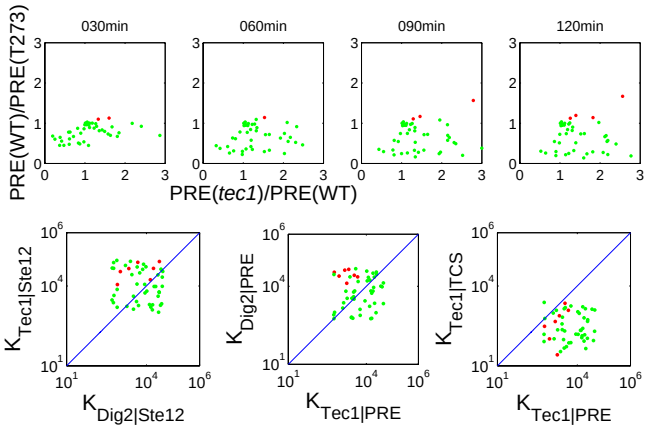

Figure S10. The correlation between affinity rates, with different initial amounts of PRE and TCSs. (A) The initial amounts of PREs and TCSs are given in the Table 1 but the initial Ste12 amount is 0.005 μM; 50 sample points; 200 nM induced pheromone; the same Fus3 activation rates; (B) the initial amount of PRE and TCS is 10% of (A) with other conditions being the same; (C) the initial amount of PRE and TCS is 1% of (A) with other conditions being the same.

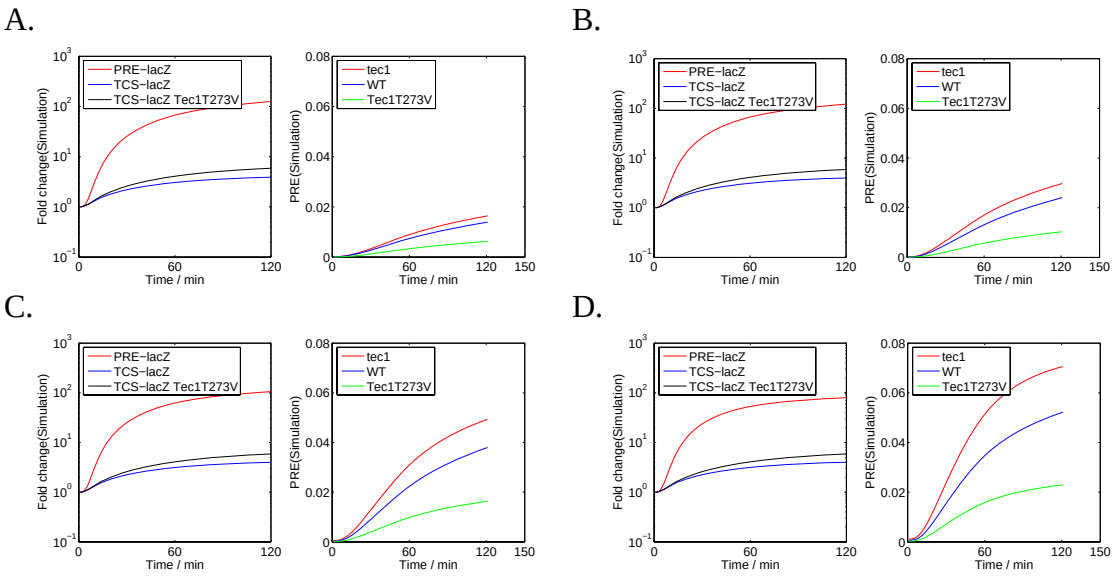

Figure S11. The effect of different ratios of w_d over v_d on the PRE outputs for four cases: (A) $w_d = 0.5v_d$; (B) $w_d = v_d$; (C) $w_d = 2.0v_d$; (D) $w_d = 4.0v_d$; The other parameters used for these cases are the same as in Figure 1D.